

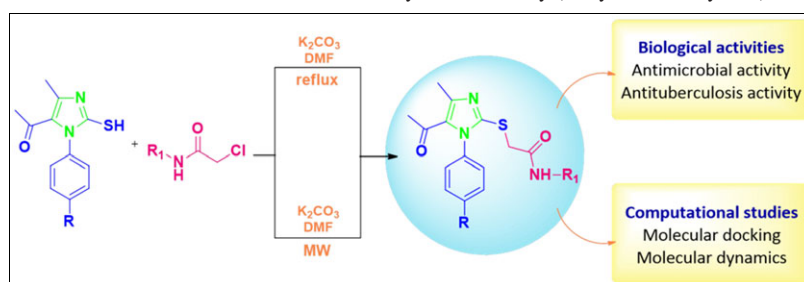
^aDepartment of Chemistry, School of Sciences, Gujarat University, Navarangpura, Gujarat, India^bMicrocare laboratory and TRC, Surat, India

*E-mail: drhiteshpatel1@gmail.com

Received June 20, 2018

DOI 10.1002/jhet.3429

Published online 00 Month 2018 in Wiley Online Library (wileyonlinelibrary.com).



Substituted imidazole analogues 2-((5-acetyl-4-methyl-1-phenyl-1*H*-imidazole-2-yl)thio)-*N*-phenylacetamides (**3a–3m**) have been synthesized from 1-[1-(phenyl)-2-mercapto-4-methyl-1*H*-imidazol-5-yl]-ethanone (**1a–1e**) and 2-chloro-*N*-phenylacetamide (**2a–2i**) in the presence of potassium carbonate as a catalyst in dimethylformamide under microwave irradiation as well as conventional method. Structures of the obtained compounds have been confirmed by advance spectroscopic techniques such as IR, ¹H NMR, ¹³C NMR, and mass spectrometry. All the synthesized compounds were tested for their *in vitro* antimicrobial and antituberculosis activities. Good antibacterial molecules were further screened for the bacterial resisted cell line, from which compound **3b** shows maximum inhibition. *In silico* molecular docking study was carried out to discover the binding affinity of synthesized compounds with active site of transferase (PDB ID: 1HNJ) and antibiotic resistance (PDB ID: 1W3R) protein. Moreover, molecular dynamics study of the **3b**-1W3R complex has also been performed, as **3b** has a good antibacterial activity as compared with other.

J. Heterocyclic Chem., **00**, 00 (2018).

INTRODUCTION

There is an enormous disease caused by bacteria and fungi. So, millions of people are infected by bacteria and fungi. Therefore, numbers of antimicrobial drug have been invented, which play an important role in treating infections [1]. World Health Organization has listed that antimicrobial resistance is one of the biggest threats to global health today [2]. There are millions of deaths occur because of the infections caused by multidrug-resistant bacteria such as MRSA, vancomycin-resistant Enterococci, drug-resistant *Pseudomonas aeruginosa* and *Acinetobacter spp.* [3,4]. Among the bacterial pathogens, *Staphylococcus aureus* is developed as a significant burden to health care authorities worldwide. Isolated strains of *Staphylococcus aureus* have showed resistance to several classes of antibacterial drugs like β -lactam antibiotics, macrolides, fluoroquinolones, glycopeptides, and oxazolidinones [2]. However, unreasonable usages of antimicrobials drive microorganisms to resistance that creates very serious clinical problems. There is a growing threat that antimicrobial resistance drugs may not be available for the treatment of common infection [5]. For this purpose, researchers need to find new antimicrobial compounds for the resistance strains [6].

Azole-based antibacterial and antifungal agents have been extensively studied a great deal as drug candidates, and some of them have been used in the medical science, which suggests the great development value of azole compounds, for example, antifungal agents like ketoconazole (1), miconazole (2), clotrimazole (3), parconazole (4), eberconazole (5), lanoconazole (6), fenticonazole (7), bifonazole (8), sulconazole (9), and sertaconazole (10) [7] (Fig. 1). Moreover, antibacterial agents are nitroimidazoles such as metronidazole (11), tinidazole, and ornidazole [8]. Among the azole, substituted imidazoles are an important class of biologically active N-containing heterocycles. Imidazole derivatives as antimicrobial agents have been investigated very well and shown large potentiality in medicinal chemistry [9–14]. The imidazole derivatives have various kind of biological activities such as antimicrobial, antituberculosis, analgesic, antimalarial, anti-HIV, and anticancer [15].

Therefore, in present study, we reported a novel series of imidazole derivatives, to combine and exploit pharmacological activities. All the target compounds were initially subjected to antimicrobial and antituberculosis activity *in vitro*. The results showed that most of the

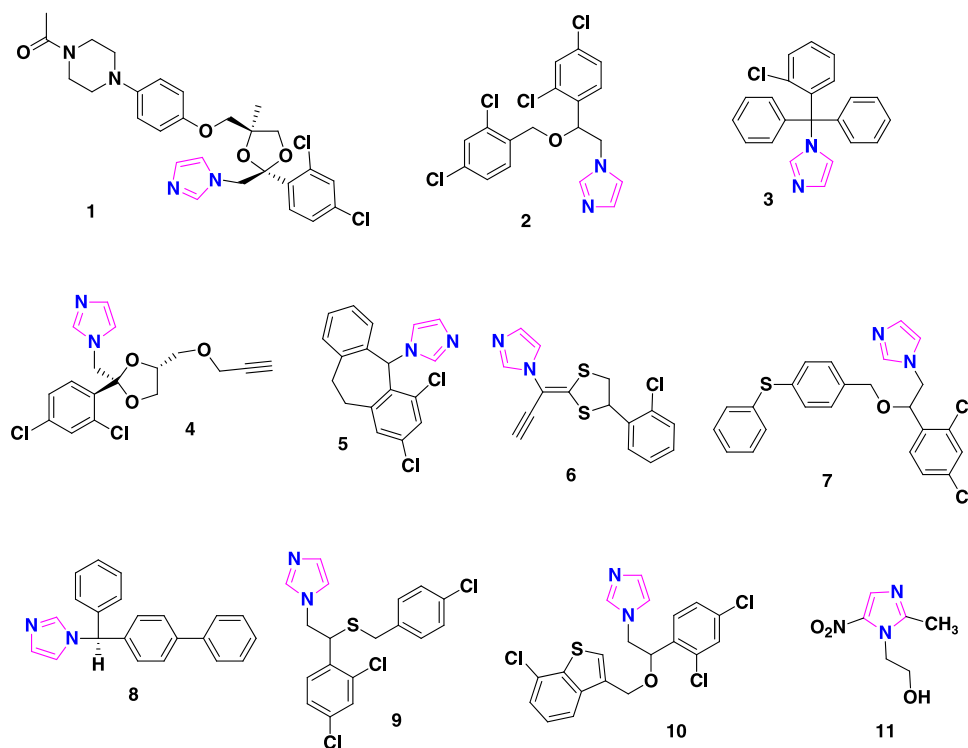


Figure 1. Structure of marketed drugs based on imidazole. [Color figure can be viewed at wileyonlinelibrary.com]

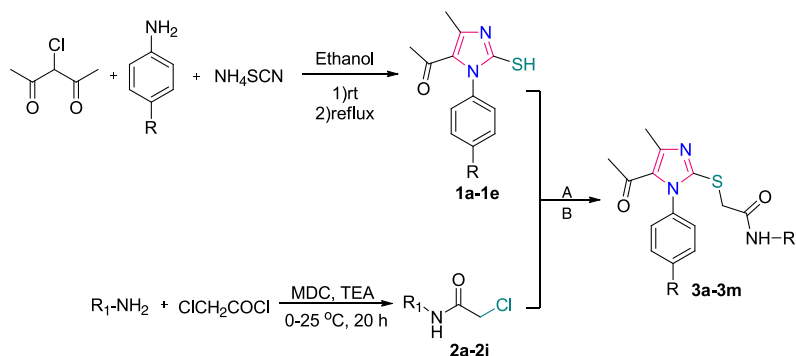
compounds displayed potent antibacterial activity against the selected cell lines. Besides, these inspiring antibacterial results encouraged us to explore their antibacterial resistance cell line. Finally, molecular docking and molecular dynamic studies suggested to perfect binding and stability position of ligand with protein, respectively.

RESULT AND DISCUSSION

Chemical synthesis. The synthetic pathway to target compounds **3a–3m** are shown in Scheme 1. Initial

compounds 1-[1-(substituted phenyl)-2-mercapto-4-methyl-1*H*-imidazol-5-yl]-ethanone was obtained from aryl amines, 3-chloro-2,4-pentanedione, and potassium thiocyanate according to previously described method (**1a–1e**) [16]. Second substituted 2-chloro-*N*-phenylacetamides compounds were obtained from aryl amines and chloroacetyl chloride according to previously described method (**2a–2i**) [17]. The targeted compounds in good yield were obtained by the reaction between 1-[1-(substituted phenyl)-2-mercapto-4-methyl-1*H*-imidazol-5-yl]-ethanones, substituted 2-chloro-*N*-phenylacetamides, and potassium carbonate as catalyst in dimethylformamide (DMF) under conventional reflux and microwave

Scheme 1. Synthetic route of 2-((5-acetyl-4-methyl-1-phenyl-1*H*-imidazol-2-yl)thio)acetamide derivatives. [Color figure can be viewed at wileyonlinelibrary.com]



irradiation condition. However, microwave irradiation condition is more preferable as compare with conventional reflux. There is mechanism shown in Figure 2. As shown in Table 1, all the synthesized compounds were proved to be efficient to generate product in good yield and mentioned with their melting points.

Spectral analysis of compound 3a. Synthesized novel substituted 2-((5-acetyl-4-methyl-1-phenyl-1*H*-imidazol-2-yl)thio)acetamide derivatives were characterized by IR, ^1H NMR, ^{13}C NMR, mass spectroscopy, and melting points after purification by crystallization using appropriate solvents. The IR spectrum of **3a** showed absorption at 3282 cm^{-1} which is due to the $-\text{N}-\text{H}$ stretching of amide and 1611 cm^{-1} is due to $-\text{C}=\text{O}$ stretching of amide. The compound showed absorption at 640 cm^{-1} , which is due to $-\text{C}-\text{S}$ stretching. The band appeared at 1670 cm^{-1} is due to $-\text{C}=\text{O}$ stretching of ketone group which confirmed the structure of the compound. The ^1H NMR spectrum of **3a** showed $\delta = 10.311$ (s, 1H, NH); 7.650–7.133 (m, 4H, Ar); 4.734 (s, 2H, CH_2); 2.463 (s, 3H, COCH_3); and 2.343 (s, 3H, CH_3). The mass spectrum of **3a** showed a molecular ion peak at m/z for 417.8 $[\text{M}]^+$, 419.9 $[\text{M} + 2]^+$. In addition, ^{13}C NMR peak at 166.18, 143.08, and 156.94 confirm

the carbons of $\text{C}=\text{O}$, $\text{C}-\text{N}$ amide group, and $\text{C}-\text{S}$, respectively, which confirmed that the molecular formula $\text{C}_{20}\text{H}_{17}\text{ClFN}_3\text{O}_2\text{S}$.

As shown in Table 2, all the synthesized molecules were tested for their antimicrobial and antituberculosis activities. Their antibacterial activity of all the compounds were compared with standard drugs such as chloroamphenicol, ciprofloxacin, and ampicillin; all the compounds are active against *Staphylococcus aureus*; compounds **3a–3e** and **3h–3j** show comparatively good inhibition in *Escherichia coli* and *Pseudomonas aeruginosa* strains, while **3b** shows good activity against *Streptococcus pyogenes* too. In addition, **3a–3d**, **3f–3j**, and **3m** show good inhibitory results against *Candida albicans* when compared with griseofulvin. All the tested molecules were not showed good activity against the *M. tuberculosis* (Fig. 3).

Compounds **3b**, **3d**, **3h**, and **3j** were screened against resisted cell line of ESBL and MRSA. From the results (Table 3), we found that compounds **3b**, **3d**, and **3h** display good activity against the ESBL cell line, while **3b** shows good inhibition against MRSA.

Docking studies were performed to explain *in silico* antibacterial studies, a protein transferase (PDB ID: 1HNJ),

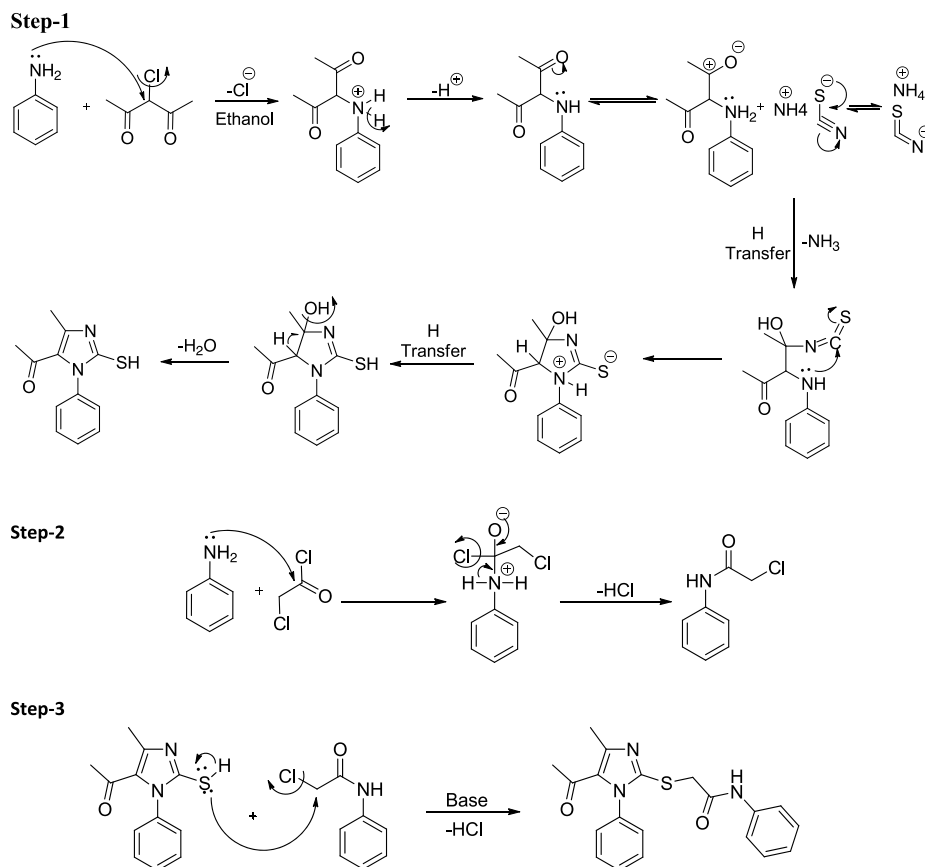


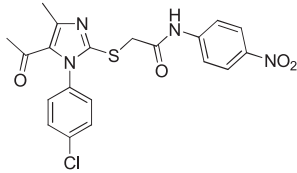
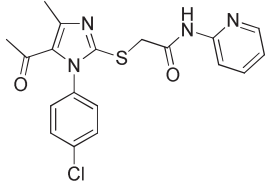
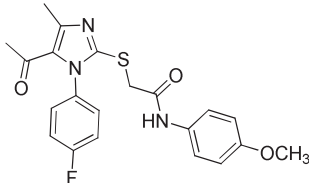
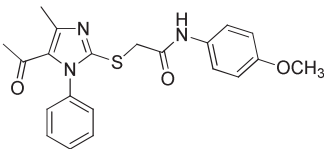
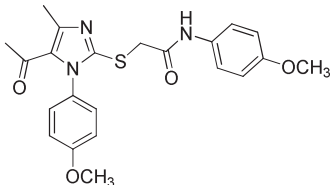
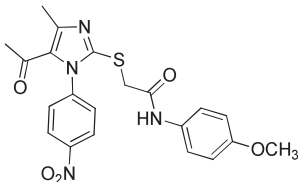
Figure 2. Mechanism route of 2-((5-acetyl-4-methyl-1-phenyl-1*H*-imidazol-2-yl)thio)acetamide derivatives.

Table 1
Synthesized 2-((5-acetyl-4-methyl-1-phenyl-1*H*-imidazol-2-yl)thio)acetamide derivatives.

Entry	Compound code	R	R ₁	Product	Yield (%) ^a	mp (°C) ^b
1	3a	Cl	4-FPh		81	179.5
2	3b	Cl	4-ClPh		65	191.2
3	3c	Cl	Ph		76	156.9
4	3d	Cl	3-OHPh		65	92.8
5	3e	Cl	4-OCH ₃ Ph		80	208.4
6	3f	Cl	4-BrPh		85	192.6
7	3g	Cl	2-Benzothiazole		25	115.8
8	3h	Cl	4-NO ₂ Ph		59	216.4

(Continues)

Table 1
(Continued)

Entry	Compound code	R	R ₁	Product	Yield (%) ^a	mp (°C) ^b
						
9	3i	Cl	2-Pyridine		66	78.6
10	3j	F	4-OCH ₃ Ph		70	171.6
11	3k	H	4-OCH ₃ Ph		68	178.3
12	3l	OCH ₃	4-OCH ₃ Ph		82	143.4
13	3m	NO ₂	4-OCH ₃ Ph		74	172.4

^aIsolated yield.

^bMelting point.

and antibiotic resistance (PDB ID: 1W3R) were identified as the target for antibacterial and resisted compounds. The molecular docking studies have been carried out to evaluate the binding affinity of **3a–3m** compounds with this receptor, which results are shown in Table 4. The most potent bacterial compounds **3b**, **3d**, **3i**, and **3j** showed good binding affinity with transferase and have binding

energy -6.28 , -6.67 , -5.58 , and -5.44 kcal/mol, respectively. Compounds **3d**, **3h**, and **3j** appeared with a good binding affinity with antibiotic resistance compared with other compounds in terms of docking score as -2.484 , -2.316 , and -2.268 kcal/mol, respectively. Binding of the ligands with proteins interaction is shown in Table 5, and figure of docking is shown in Fig. 4.

Table 2
Biological activity.

Entry	Compound code	Antibacterial activity				Antifungal activity			Antituberculosis activity
		MIC ^a µg/mL				MFC ^b µg/mL			MIC ^a µg/mL
		EC ^c	PA ^d	SA ^e	SP ^f	CA ^g	AN ^h	AC ⁱ	
1	3a	62.5	125	100	250	500	500	1000	100
2	3b	12.5	50	12.5	50	250	1000	500	62.5
3	3c	25	50	12.5	125	500	250	250	125
4	3d	25	50	12.5	125	250	500	1000	100
5	3e	12.5	50	250	250	1000	250	250	250
6	3f	125	100	62.5	50	500	1000	1000	100
7	3g	250	125	62.5	62.5	500	1000	1000	62.5
8	3h	12.5	125	50	100	250	500	500	50
9	3i	62.5	62.5	100	62.5	250	500	250	50
10	3j	12.5	62.5	62.5	62.5	500	500	>1000	125
11	3k	125	125	250	500	1000	>1000	>1000	62.5
12	3l	125	100	125	250	>1000	>1000	>1000	250
13	3m	250	100	125	250	500	>1000	>1000	100
14	Gentamycine ^j	0.05	1	0.25	0.5	—	—	—	—
15	Ampicillin ^j	100	—	250	100	—	—	—	—
16	Chloramphenicol ^j	50	50	50	50	—	—	—	—
17	Ciprofloxacin ^j	25	25	50	50	—	—	—	—
18	Norfloracin ^j	10	10	10	10	—	—	—	—
19	Nystatin ^j	—	—	—	—	100	100	100	—
20	Griseofulvin ^j	—	—	—	—	500	100	100	—
21	Isoniazid ^j	—	—	—	—	—	—	—	0.20

^aMinimum inhibition concentration.

^bMinimum fungicidal concentration.

^c*Escherichia coli* (MTCC 443).

^d*Pseudomonas aeruginosa* (MTCC 1688).

^e*Staphylococcus aureus* (MTCC 96).

^f*Streptococcus pyogenes* (MTCC 442).

^g*Candida albicans* (MTCC 227).

^h*Aspergillus niger* (MTCC 282).

ⁱ*Aspergillus clavatus* (MTCC 1323).

^jStandard drug.

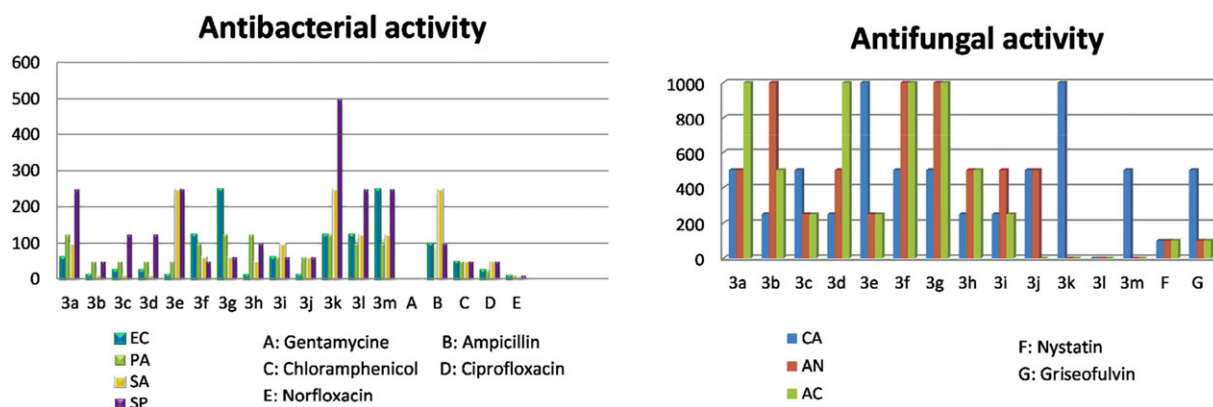


Figure 3. Graphical representations of antibacterial activity and antifungal activity. [Color figure can be viewed at wileyonlinelibrary.com]

Structure–activity relationship. The substitution patterns of the aryl amine ring at the different positions were observed to affect biological activity. The substitutions on phenyl ring attached to imidazole were also observed to affect biological activity. The electronic nature of the

substituents led to significant variation for disparity in activity. Compounds possess electron-donating and withdrawing substituents on both of the phenyl rings. Halogenated groups (–Cl and –F) at 4th position of the phenyl ring attached to imidazole led to an increase in the

Table 3
Activity against resisted cell line.

Entry	Compound code	Antibacterial activity	
		MIC ^a µg/mL	
		ESBL ^b	MRSA ^c
1	3b	50	12.5
2	3d	62.5	100
3	3h	50	250
4	3j	250	500

^aMinimum inhibition concentration.

^bExtended-spectrum *beta*-lactamases.

^cMethicillin-resistant *Staphylococcus aureus*.

Table 4
Binding score.

Entry	Compound code	Transferase ^a (kcal/mol)	Antibiotic resistance ^b (kcal/mol)
1	3a	-6.05	-1.151
2	3b	-6.28	-1.736
3	3c	-5.61	-1.634
4	3d	-6.67	-2.484
5	3e	-4.75	-2.115
6	3f	-6.31	-1.496
7	3g	-6.28	-1.235
8	3h	-4.83	-2.316
9	3i	-5.85	-1.758
10	3j	-5.44	-2.268
11	3k	-6.03	-2.018
12	3l	-4.95	-2.045
13	3m	-3.08	-2.181
14	Ampicillin ^c	-6.04	—
15	Chloramphenicol ^c	-6.89	—
16	Ciprofloxacin ^c	-4.40	—
17	Metronidazole ^c	—	-2.670

^aPDB of 1HNJ.

^bPDB of 1W3R.

^cStandard drug.

antibacterial activity. The methoxy group (weak electron donating) at 4th position of both phenyl rings was found to be less active. As seen from Table 5, **3b**, **3d**, and **3h** corresponding aryl moieties align well and interact with protein residues by dispersion interactions except **3j**. This could be one of the reasons of **3j** being less scored and less active *in vitro* for resisted cell line. In a similar manner, we tried to also hypothesize the differential activities between structurally close homologs: **3e**, **3k**, **3l**, and **3m**. It was evident to see that bulky substitution was not tolerated at C-4 position of the phenyl ring. Indeed, as seen from Figure 4, compounds **3b**, **3d**, and **3h** with imidazole fit well in the protein allowing the aryl ring to have dispersion (π - π) interactions with neighboring residues. Increasing the bulk from methoxy **3e**, **3k**, **3l**, and **3m** moved the phenyl ring slightly out of the hydrophobic pocket facing the solvent side on account of steric clashes. Indeed, this was reflected in the reduced/loss of activity of **3e**, **3k**, **3l**, and **3m**. Both phenyl rings with chloro group showed higher antibacterial inhibitory activity. Furthermore, compounds having electron-donating substituents ($-\text{OCH}_3$) at 4th position of phenyl ring to a decrease in the antibacterial inhibition activity, except halogenated groups ($-\text{Cl}$, $-\text{Br}$, and $-\text{F}$). In addition, compound possessing $-\text{OH}$ group at 3rd position of phenyl ring led to an increase in the antibacterial inhibition activity. Compounds bearing benzothiazole and pyridine at R₁ position possessed good activity. Among, halogenated substituted amine aryl ring, the chloro-substituted group was more potent compared to bromo and fluoro substituted group. Most of the compounds succeeded to inhibit lead in antibacterial activity strain *Staphylococcus aureus*. Moreover, chloro-substituted group on both of the phenyl rings were showed higher activity against resisted cell line. This concept had been explained graphically in Figure 5.

Molecular dynamics simulation. Molecular dynamics is a useful tool to study the interaction simulation between protein and inhibitor. As per the docking score,

Table 5
Various ligands and proteins interaction.

Compound code	Protein	H-bond		π - π interaction	Salt bridge
		H bond formation by amino acid	H bond formation by ligand		
3b	Transferase (1HNJ)	ASN 247 to O	NH to GLY 209	Phenyl ring (attached imidazole) to PHE 213	—
3d		—	—	Phenyl ring (attached imidazole) to PHE 213	CYS 112, ASN 274
3h	Antibiotic resistance	ARG 17 to O	NH to SER 13	Imidazole to TRP 26	—
3j	(1W3R)	ARG 17 to O	NH to SER 13	—	—

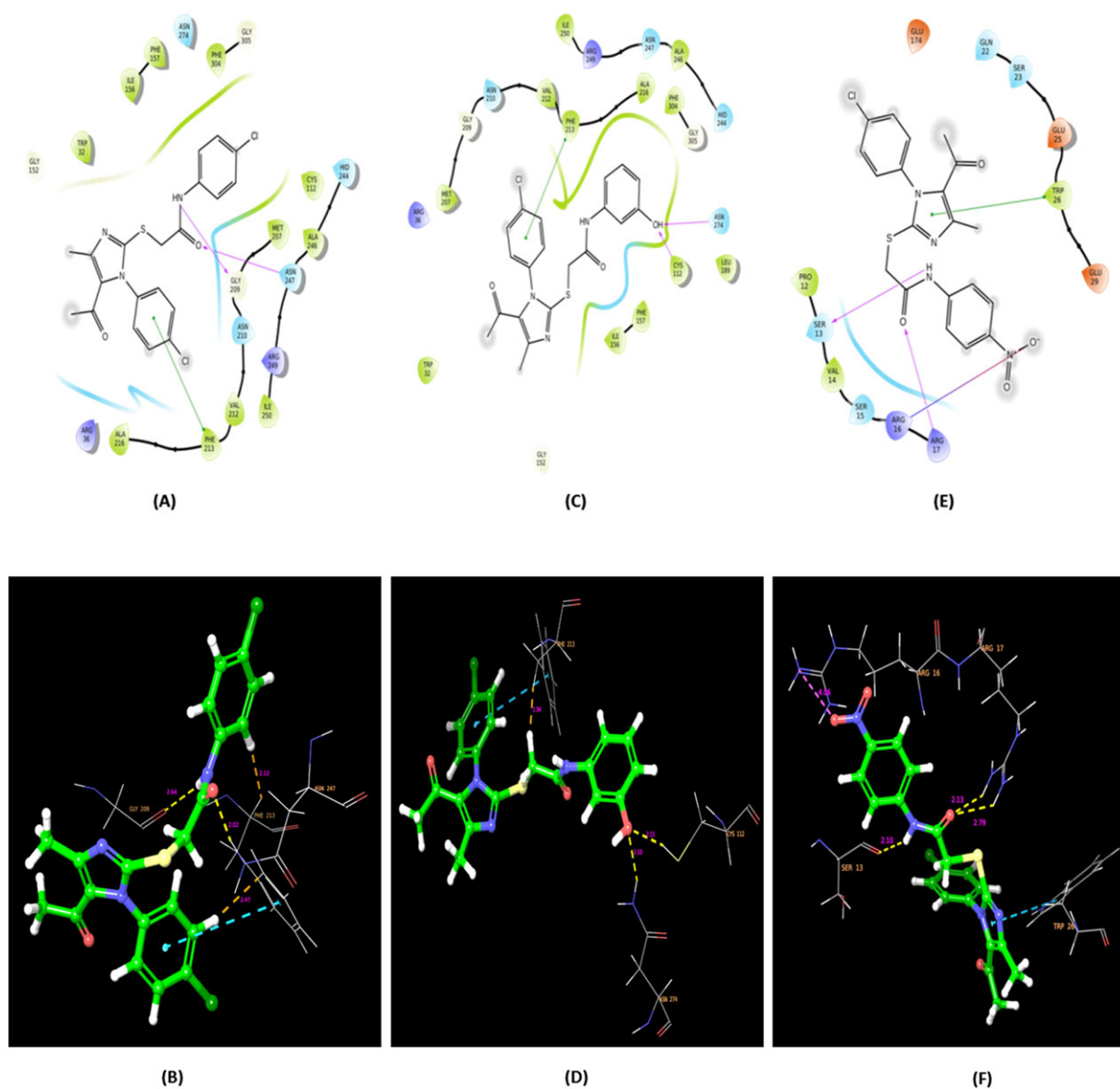


Figure 4. (A), (C), and (E) are 2D binding pose and (B), (D), and (F) are 3D binding pose of compounds **3b**, **3d**, and **3h**, respectively. [Color figure can be viewed at wileyonlinelibrary.com]

compound **3b** has the good binding energy when it was interacted with antibiotic resistance (1W3R) protein computationally. Molecular dynamics simulation was performed to find the best equilibrium conformation of **3b**-1W3R complex. The study indicates that **3b** formed interaction with protein (Fig. 6). There were found 22 binding site residues interaction between 1W3R and compound **3b** (Fig. 7). Table 6 showed the molecular interaction profile of the compound with protein. According to the force applied during the simulation, **3b** got continuously fluctuated and yield 0.5 Å–8.5 Å RMSD values (Fig. 8). These RMSD values suggest that

the protein structure is unstable during most of the simulation time. In addition to this, the other tested MD result also suggests that the protein structure remains unstable during most of the simulation (Fig. 9).

EXPERIMENTAL

Here, reaction was carried out in a CEM Discover microwave system as well as modified Samsung microwave oven. Completion of reaction and purity of all compounds were checked on aluminum-coated thin

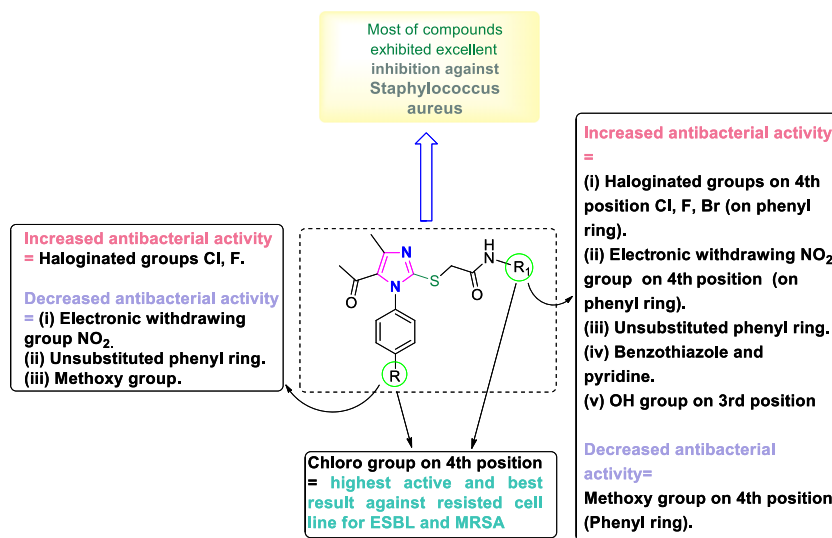


Figure 5. Structure–activity relationship. [Color figure can be viewed at wileyonlinelibrary.com]

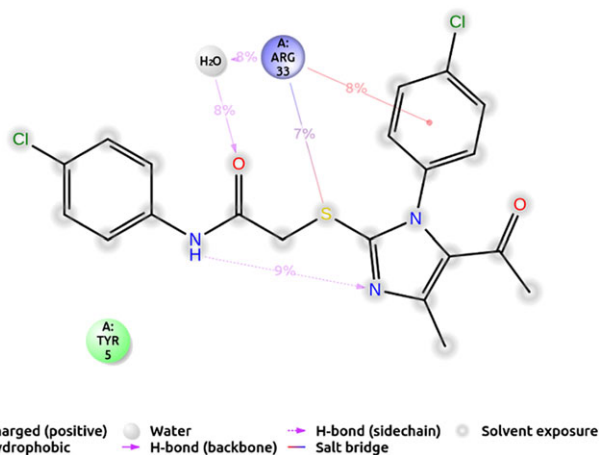


Figure 6. Ligand interaction pattern with percentage of contacts of the ligand against 1W3R during complete 10 ns explicit molecular dynamics simulation. [Color figure can be viewed at wileyonlinelibrary.com]

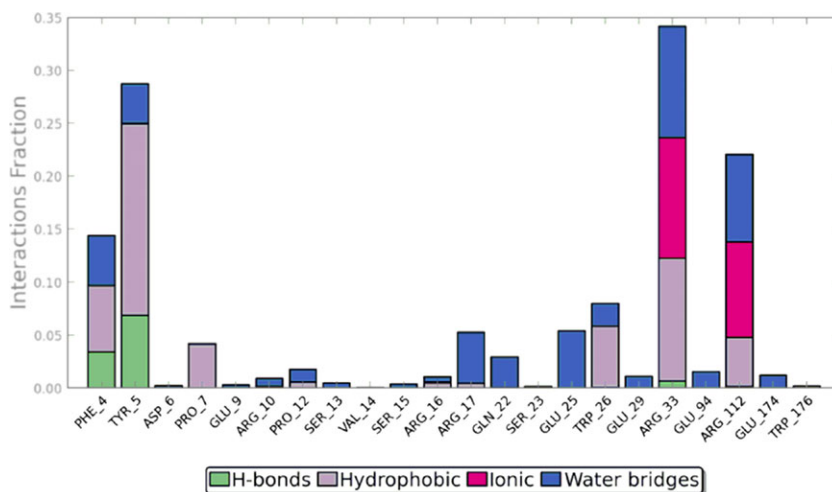


Figure 7. Bar representation of the conserved binding site residues that influenced ligand against the 1W3R during 10 ns molecular dynamics simulations. [Color figure can be viewed at wileyonlinelibrary.com]

Table 6
Protein interactions with the ligand.

Protein	Compound code	H-bond	Hydrophobic interaction	Ionic bonds	Water bridges
Antibiotic resistance (1W3R)	3b				PHE-4 TYR-5 PRO-7 PRO-12 ARG-16
			PHE-4 TYR-5 PRO-7 PRO-12 ARG-16 ARG-17 TRP-26 GLU-29 ARG-33 ARG-112	ARG-33 ARG-112	ARG-17 SER-13 SER-15 GLN-22 SER-23 TRP-26 GLU-29 ARG-33 GLU-94 ARG-112 GLU-174 TRP-176
		PHE-4 TYR-5 ASP-6 ARG-33			

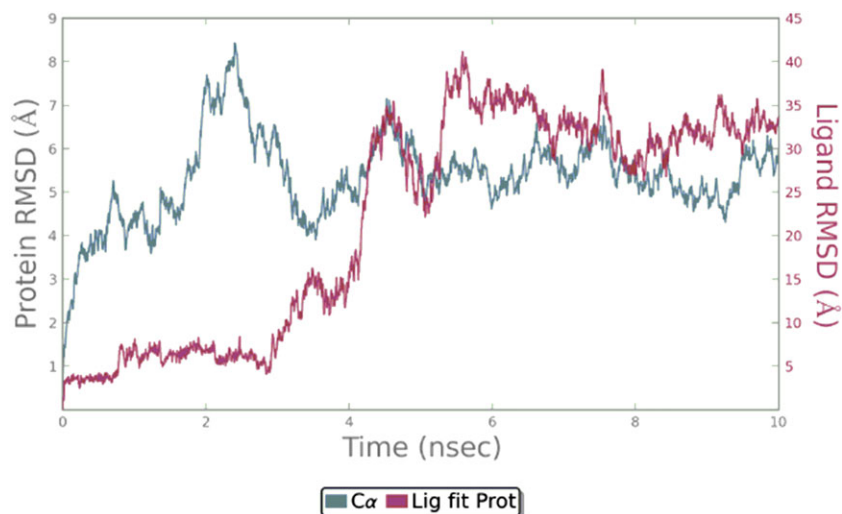


Figure 8. Graph shows the RMSD value for protein and ligand during 10 ns molecular dynamics simulations. [Color figure can be viewed at [wileyonlinelibrary.com](#)]

layered chromatographic (TLC) plates 60 F245 (E. Merck, Kenilworth, NJ) that was used as a stationary phase and hexane : ethylacetate (2.5:2.5 V/V) system utilized as mobile phase and visualized under ultraviolet light. Digital apparatus Optimelt MPA 100 was used for melting point. FT-IR spectrum was recorded on a Perkin Elmer FT-IR 377 spectrometer using KBr powder as standard. ^{13}C NMR spectra was recorded on a Bruker AV 100 MHz spectrometer using DMSO as solvent. ^1H NMR spectra was recorded on a Bruker AV 400 MHz spectrometer using DMSO- d_6 as solvent and tetramethylsilane as internal reference. Mass spectra were recorded at Advion expression CMS, USA. Molecular docking study was performed using Glide on Maestro

10.7. Desmond tool incorporated in Maestro 10.7 was used for the molecular dynamics study.

General procedure for the synthesis of 2-((5-acetyl-1-(4-chlorophenyl)-4-methyl-1H-imidazol-2-yl)thio)-N-(4-fluorophenyl)acetamide (3a). *Under reflux condition.* In round bottom flask (50 mL), a mixture of 1-[1-(4-chlorophenyl)-2-mercapto-4-methyl-1H-imidazol-5-yl]-ethanone (1 mol) and 2-chloro-N-(4-fluorophenyl)acetamide (1 mol) in DMF was reacted in the presence of potassium carbonate (2 mol) as catalyst to maintain basic condition. The reaction mixture was then refluxed for 6 h. The mixture was heated and refluxed till completion of the reaction indicated on TLC. After completion of the reaction, the reaction flask was cooled and the reaction mixture was

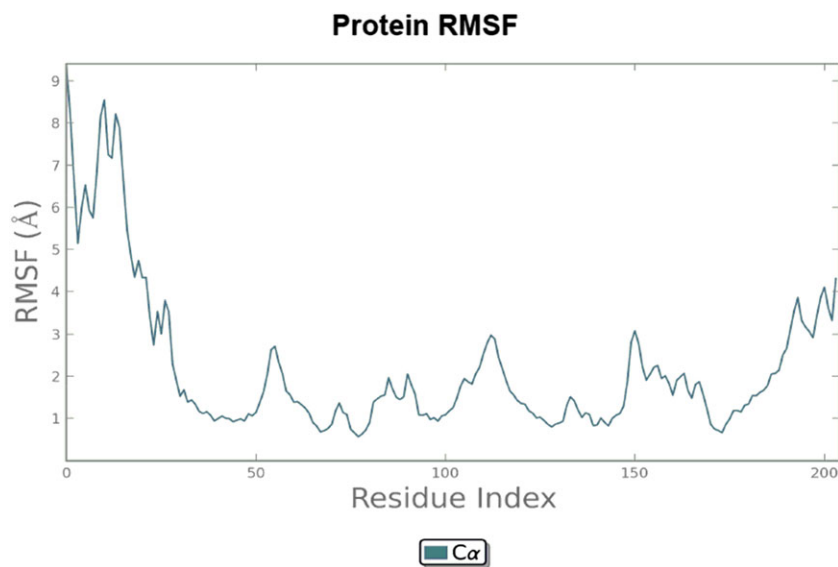


Figure 9. Graph of RMSF value for 1W3R during 10 ns molecular dynamics simulations. [Color figure can be viewed at wileyonlinelibrary.com]

diluted with water. The precipitates were filtered and recrystallized from ethanol. All the other derivatives were synthesized using the same procedure for variation time.

Under MW condition. In round bottom flask (50 mL), a mixture of 1-[1-(4-chlorophenyl)-2-mercapto-4-methyl-1H-imidazol-5-yl]-ethanone (1 mol) and 2-chloro-*N*-(4-fluorophenyl)acetamide (1 mol) in DMF was reacted in the presence of potassium carbonate (0.5 mol) as catalyst to maintain basic condition. The reaction mixture was exposed to MW irradiation at 450 W for 2 min. The mixture was heated and refluxed till completion of the reaction, the reaction was monitored by TLC. After completion of the reaction, the reaction flask was cooled and the reaction mixture was diluted with water. The precipitates were filtered and recrystallized from ethanol. All the other derivatives were synthesized using the same procedure variation time.

Spectral analysis. Synthesized compounds were confirmed through different spectroscopic methods like ^{13}C NMR, ^1H NMR, mass, and IR spectroscopy. Compounds **3a–3m** were analyzed via ^1H NMR, mass, and IR spectroscopy. Compounds **3a**, **3f**, and **3h** were further characterized by using ^{13}C NMR.

2-((5-Acetyl-1-(4-chlorophenyl)-4-methyl-1H-imidazol-2-yl)thio)-*N*-(4-fluorophenyl)acetamide (3a). Yield: 81%. MW: 417.88 g/mol. MF: $\text{C}_{20}\text{H}_{17}\text{ClFN}_3\text{O}_2\text{S}$; mp: 179.5°C. IR (KBr) λ_{max} (cm^{-1}): 3282, 2876, 2767, 1670, 1611, 1504, 1373, 1221, 1096, 967, 838, 787, 685, 640, 513. ^1H NMR (400 MHz, $\text{DMSO}-d_6$): δ (ppm) = 10.311 (s, 1H, NH); 7.650–7.133 (m, 8H, Ar); 4.734 (s, 2H, CH_2); 2.463 (s, 3H, COCH_3); 2.343 (s, 3H, CH_3). ^{13}C NMR (100 MHz, DMSO): δ (ppm) = 18.43, 29.53, 29.71, 55.02, 115.26, 115.48, 120.78, 120.86, 122.80, 123.30, 128.44, 129.44, 129.98, 132.23, 135.08, 143.08, 156.94,

159.21, 166.18, 169.77, 188.93. Mass (m/z): 417.8 $[\text{M}]^+$, 419.1 $[\text{M} + 2]^+$, 420.1 $[\text{M} + 3]^+$.

2-((5-Acetyl-1-(4-chlorophenyl)-4-methyl-1H-imidazol-2-yl)thio)-*N*-(4-chlorophenyl)acetamide (3b). Yield: 65%. MW: 434.34 g/mol. MF: $\text{C}_{20}\text{H}_{17}\text{Cl}_2\text{N}_3\text{O}_2\text{S}$; mp: 191.2°C. IR (KBr) λ_{max} (cm^{-1}): 3222, 3176, 3074, 2999, 2957, 1612, 1558, 1503, 1423, 1372, 1213, 1177, 1071, 990, 934, 831, 736. ^1H NMR (400 MHz, $\text{DMSO}-d_6$): δ (ppm) = 10.399 (s, 1H, NH); 7.647–7.359 (m, 8H, Ar); 4.744 (s, 2H, CH_2); 2.458 (s, 3H, COCH_3); 2.342 (s, 3H, CH_3). Mass (m/z): 434.7 $[\text{M}]^+$, 435.86 $[\text{M} + 1]^+$, 436.85 $[\text{M} + 2]^+$.

2-((5-Acetyl-1-(4-chlorophenyl)-4-methyl-1H-imidazol-2-yl)thio)-*N*-phenylacetamide (3c). Yield: 76%. MW: 399.89 g/mol. MF: $\text{C}_{20}\text{H}_{18}\text{ClN}_3\text{O}_2\text{S}$; mp: 156.9°C. IR (KBr) λ_{max} (cm^{-1}): 3302, 3205, 3093, 2774, 1668, 1609, 1548, 1488, 1370, 1260, 1090, 943, 844, 690. ^1H NMR (400 MHz, $\text{DMSO}-d_6$): δ (ppm) = 10.863 (s, 1H, NH); 7.632–7.670 (t, 2H, Ar); 7.600–7.578 (d, 1H, Ar, $J = 8.8$); 7.389–7.426 (t, 2H, Ar); 7.33–7.29 (t, 2H, Ar); 7.04–7.00 (t, 2H, Ar); 6.958–6.980 (d, 1H, Ar, $J = 8.8$); 4.746 (s, 2H, CH_2); 2.465 (3H, COCH_3); 2.344 (s, 3H, CH_3). Mass (m/z): 399.7 $[\text{M}]^+$, 400.8 $[\text{M} + 1]^+$, 401.7 $[\text{M} + 2]^+$.

2-((5-Acetyl-1-(4-chlorophenyl)-4-methyl-1H-imidazol-2-yl)thio)-*N*-(3-hydroxyphenyl)acetamide (3d). Yield: 65%. MW: 415.89 g/mol. MF: $\text{C}_{20}\text{H}_{18}\text{ClN}_3\text{O}_3\text{S}$; mp: 92.8°C. IR (KBr) λ_{max} (cm^{-1}): 3206, 3177, 3075, 2958, 1666, 1599, 1558, 1525, 1374, 1339, 1213, 990, 902, 735. ^1H NMR (400 MHz, $\text{DMSO}-d_6$): δ (ppm) = 10.113 (s, 1H, NH); 9.407 (s, 1H, OH); 7.643–6.443 (m, 8H, Ar); 4.714 (s, 2H, CH_2); 2.463 (s, 3H, COCH_3); 2.343 (s, 3H, CH_3). Mass (m/z): 416.07 $[\text{M} + 1]^+$, 417.80 $[\text{M} + 2]^+$.

2-((5-Acetyl-1-(4-chlorophenyl)-4-methyl-1H-imidazol-2-yl)thio)-*N*-(4-methoxyphenyl)acetamide (3e). Yield: 80%. MW: 429.92 g/mol. MF: $\text{C}_{21}\text{H}_{20}\text{ClN}_3\text{O}_3\text{S}$; mp: 208.4°C.

IR (KBr) λ_{\max} (cm⁻¹): 3287, 3068, 2896, 2767, 1676, 1491, 1372, 1309, 1256, 1096, 961, 832, 728. ¹H NMR (400 MHz, DMSO-*d*₆): δ (ppm) = 10.107 (s, 1H, NH); 7.651–7.504 (m, 4H, Ar); 7.499–7.482 (d, 2H, Ar, *J* = 6.8); 6.894–6.871 (d, 2H, Ar, *J* = 9.2); 4.711 (s, 2H, CH₂); 3.715 (s, 3H, OCH₃); 2.466 (s, 3H, COCH₃); 2.343 (s, 3H, CH₃). Mass (*m/z*): 429.7 [M]⁺, 430.8 [M + 2]⁺, 431.7 [M + 3]⁺.

2-((5-Acetyl-1-(4-chlorophenyl)-4-methyl-1H-imidazol-2-yl)thio)-N-(4-bromophenyl)acetamide (3f). Yield: 85%. MW: 478.79 g/mol. MF: C₂₀H₁₇BrClN₃O₂S; mp: 192.6°C. IR (KBr) λ_{\max} (cm⁻¹): 3323, 3242, 3194, 3123, 3063, 2847, 2774, 1710, 1538, 1415, 1396, 1334, 1302, 1244, 1218, 1189, 1071, 967, 908, 831, 714, 681, 574. ¹H NMR (400 MHz, DMSO-*d*₆): δ (ppm) = 10.396 (s, 1H, NH); 7.647–7.484 (m, 8H, Ar); 4.745 (s, 2H, CH₂); 2.459 (s, 3H, COCH₃); 2.342 (s, 3H, CH₃). ¹³C NMR (100 MHz, DMSO): δ (ppm) = 18.43, 29.53, 55.10, 114.98, 120.99, 122.79, 123.33, 128.44, 129.44, 129.99, 131.61, 132.26, 138.03, 143.06, 156.92, 166.49, 169.73, 188.93. Mass (*m/z*): 479.6 [M + 1]⁺.

2-((5-Acetyl-1-(4-chlorophenyl)-4-methyl-1H-imidazol-2-yl)thio)-N-(benzo[d]thiazol-2-yl)acetamide (3g). Yield: 25%. MW: 456.97 g/mol. MF: C₂₁H₁₇ClN₄O₂S₂; mp: 115.8°C. IR (KBr) λ_{\max} (cm⁻¹): 3189, 3066, 2992, 2770, 1709, 1651, 1608, 1548, 1490, 1370, 1320, 1268, 1182, 1019, 972, 837, 757, 642, 511. ¹H NMR (400 MHz, DMSO-*d*₆): δ (ppm) = 7.971 (s, 1H, NH); 7.770–7.293 (m, 8H, Ar); 4.918 (s, 2H, CH₂); 2.447 (s, 3H, COCH₃); 2.346 (s, 3H, CH₃). Mass (*m/z*): 456.5 [M]⁺.

2-((5-Acetyl-1-(4-chlorophenyl)-4-methyl-1H-imidazol-2-yl)thio)-N-(4-nitrophenyl)acetamide (3h). Yield: 59%. MW: 444.89 g/mol. MF: C₂₀H₁₇ClN₄O₄S; mp: 216.4°C. IR (KBr) λ_{\max} (cm⁻¹): 3288, 3158, 3098, 2950, 1714, 1609, 1555, 1413, 1371, 1257, 1204, 1185, 1015, 848, 745, 640, 576. ¹H NMR (400 MHz, DMSO-*d*₆): δ (ppm) = 10.896 (s, 1H, NH); 8.248–8.225 (d, 2H, Ar, *J* = 9.2); 7.854–7.831 (d, 2H, Ar, *J* = 9.2); 7.657–7.588 (m, 4H, Ar); 4.820 (s, 2H, CH₂); 2.456 (s, 3H, COCH₃); 2.345 (s, 3H, CH₃). ¹³C NMR (100 MHz, DMSO): δ (ppm) = 18.41, 29.51, 29.70, 55.20, 118.81, 122.79, 123.43, 125.05, 128.41, 129.44, 130.03, 132.33, 142.30, 142.99, 144.76, 156.87, 167.47, 169.62, 188.98. Mass (*m/z*): 444.5 [M]⁺, 446.5 [M + 2]⁺.

2-((5-Acetyl-1-(4-chlorophenyl)-4-methyl-1H-imidazol-2-yl)thio)-N-(pyridin-2-yl)acetamide (3i). Yield: 66%. MW: 400.88 g/mol. MF: C₁₉H₁₇ClN₄O₂S; mp: 78.6°C. IR (KBr) λ_{\max} (cm⁻¹): 3277, 3197, 3083, 1608, 1515, 1403, 1373, 1236, 1174, 1086, 1030, 822, 706. ¹H NMR (400 MHz, DMSO-*d*₆): δ (ppm) = 10.804 (s, 1H, NH); 8.339–6.974 (m, 8H, Ar); 4.814 (s, 2H, CH₂); 2.437 (s, 3H, COCH₃); 2.359 (s, 3H, CH₃). Mass (*m/z*): 401.08 [M + 1]⁺.

2-((5-Acetyl-1-(4-fluorophenyl)-4-methyl-1H-imidazol-2-yl)thio)-N-(4-methoxyphenyl)acetamide (3j). Yield: 70%. MW: 413.47 g/mol. MF: C₂₁H₂₀FN₃O₃S; mp: 171.6°C.

IR (KBr) λ_{\max} (cm⁻¹): 3276, 3095, 1618, 1572, 1474, 1318, 1248, 1029, 992, 860, 748, 689. ¹H NMR (400 MHz, DMSO-*d*₆): δ (ppm) = 10.085 (s, 1H, NH); 7.680–6.869 (m, 8H, Ar); 4.689 (s, 2H, CH₂); 3.714 (s, 3H, CH₃); 2.332 (s, 3H, COCH₃); 2.087 (s, 3H, CH₃). Mass (*m/z*): 414.12 [M]⁺.

2-((5-Acetyl-4-methyl-1-phenyl-1H-imidazol-2-yl)thio)-N-(4-methoxyphenyl)acetamide (3k). Yield: 68%. MW: 395.47 g/mol. MF: C₂₁H₂₁N₃O₃S; mp: 178.3°C. IR (KBr) λ_{\max} (cm⁻¹): 3278, 3062, 2840, 2774, 1674, 1504, 1372, 1307, 1252, 1178, 1073, 1029, 830, 699, 529. ¹H NMR (400 MHz, DMSO-*d*₆): δ (ppm) = 10.065 (s, 1H, NH); 7.607–7.406 (m, 8H, Ar); 6.891–6.869 (t, 1H, Ar, *J* = 8.8); 4.717 (s, 2H, CH₂); 3.714 (s, 3H, OCH₃); 2.466 (s, 3H, COCH₃); 2.329 (s, 3H, CH₃). Mass (*m/z*): 395.7 [M]⁺, 396.6 [M + 1]⁺.

2-((5-Acetyl-1-(4-methoxyphenyl)-4-methyl-1H-imidazol-2-yl)thio)-N-(4-methoxyphenyl)acetamide (3l). Yield: 82%. MW: 425.50 g/mol. MF: C₂₂H₂₃N₃O₄S; mp: 143.4°C. IR (KBr) λ_{\max} (cm⁻¹): 3288, 3063, 2840, 2782, 1684, 1503, 1523, 1345, 1243, 1156, 1034, 846, 713, 521. ¹H NMR (400 MHz, DMSO-*d*₆): δ (ppm) = 10.047 (s, 1H, NH); 7.528–6.868 (m, 8H, Ar); 4.661 (s, 2H, CH₂); 3.793 (s, 3H, OCH₃); 3.714 (s, 3H, OCH₃); 2.459 (s, 3H, COCH₃); 2.312 (s, 3H, CH₃). Mass (*m/z*): 425.7 [M]⁺, 426.7 [M + 1]⁺.

2-((5-Acetyl-4-methyl-1-(4-nitrophenyl)-1H-imidazol-2-yl)thio)-N-(4-methoxyphenyl)acetamide (3m). Yield: 74%. MW: 440.47 g/mol. MF: C₂₁H₂₀N₄O₅S; mp: 172.4°C. IR (KBr) λ_{\max} (cm⁻¹): 3286, 3158, 2965, 1784, 1669, 1557, 1494, 1327, 1325, 1248, 1204, 1102, 1025, 867, 787, 640, 576. ¹H NMR (400 MHz, DMSO-*d*₆): δ (ppm) = 10.028 (s, 1H, NH); 7.878–6.867 (m, 8H, Ar); 4.655 (s, 2H, CH₂); 3.780 (s, 3H, OCH₃); 2.686 (s, 3H, COCH₃); 2.312 (s, 3H, CH₃). Mass (*m/z*): 440.08 [M]⁺, 441.08 [M + 1]⁺.

In vitro activity. *In vitro* antimicrobial activity of all synthesized novel substituted 2-((5-acetyl-4-methyl-1-phenyl-1H-imidazole-2-yl)thio)-N-phenylacetamide derivatives were checked against *Staphylococcus aureus*, *Escherichia coli*, *Streptococcus pyogenes*, *Pseudomonas aeruginosa* strains of antibacterial and *Candida albicans*, *Aspergillus niger*, *Aspergillus clavatus* strains of antifungal by using a method as described by S. M. Prajapati [18]. *In vitro* antituberculosis activity of all the synthesized derivatives against mycobacterium tuberculosis H37Rv strain was tested by utilizing Lowenstein–Jensen medium (conventional method) as described by A. Rattan [19].

Docking methodology. Maestro 10.7 was used to carry out molecular docking study using default settings. Protein transferase (PDB ID: 1HNJ) [20] and antibiotic resistance (PDB ID: 1W3R) [21] were employed from the protein data bank with the incorporated ligand structure in binding site [22]. Proteins were prepared in “protein preparation wizard” tool fused in Glide using default settings. All the ligands were prepared using

“LigPrep” tool, and those lower energetic conformers were used as ligands for the molecular docking. The grid was generated by using an incorporated ligand in the protein cavity, and ligand docking is performed using extra precision in Glide.

Molecular dynamics. The explicit molecular dynamics study of the ligand-receptor compounds of the identified lead against the native ligand in the antibiotic receptor was carried out using Desmond [23]. First, the aqueous solvation system of ligand receptor complex was built by system builder OPLS 2005 force field through the predefined TIP3P solvation of orthorhombic solvation boundary with box volume (8924 Å³), which was later followed by ions neutralization by addition of sodium. This system was later minimized with 2000 interactions with the convergence criteria of 1 kcal/mol/Å. The minimized explicit solvation complex of ligand-receptor complex is simulated for 10 ns using NPT ensemble [temperature (300 K) and pressure (1.01325 bar)] with a default set of relaxation before simulation.

CONCLUSION

In the present study, our main focus is to synthesize a novel series of 2-((5-acetyl-4-methyl-1-phenyl-1*H*-imidazole-2-yl)thio)acetamide derivatives using potassium carbonate as catalyst and DMF as a solvent under conventional and microwave irradiation condition. Microwave irradiation method supported several benefits compared with conventional method. All the synthesized compounds were screened for their *in vitro* antimicrobial and antituberculosis activities. Regarding biological point of view, compound **3b** shows good antibacterial activity, having the highest inhibition against ESBL and MRSA resisted cell line and having a good docking score. In molecular dynamics, compound **3b** simulation results can be shown that the compound 3b is sometimes unstable in 1W3R protein structure through the simulation time.

Acknowledgments. We are thankful to the Department of Chemistry, Gujarat University Ahmedabad, for providing the necessary facilities. UGC-Info net & INFLIBNET Gujarat University are acknowledged for providing the e-resource facilities, NFDD Centre for ¹H NMR and ¹³C NMR, and SynZeal Research Solutions for mass spectroscopy. We are thankful to Microcare laboratory for biological screening. We are very much thankful to Schrodinger team for the computational tools.

REFERENCES AND NOTES

[1] Danishuddin, M.; Kaushal, L.; Baig, M. H.; Khan, A. U. *Genomics Proteomics Bioinformatics* 2012, 10, 360.

- [2] López-Rojas, P.; Janeczko, M.; Kubiński, K.; Amesty, Á.; Maslyk, M.; Estévez-Braun, A. *Molecules* 2018, 18, 199.
- [3] Dewangan, R. P.; Bisht, G. S.; Singh, V. P.; Yar, M. S.; Pasha, S. *Bioorg Chem* 2018, 76, 538.
- [4] Chellat, M. F.; Raguž, L.; Riedl, R. *Angew Chem Int Ed* 2016, 55, 6600.
- [5] Lloyd, D. H. *Vet Dermatol* 2012, 23, 299.
- [6] Wang, X. L.; Wang, X. L.; Zhou, C. H.; Geng, R. X. *Chin J New Drug* 2010, 19, 2050.
- [7] Liu, C.; Shi, C.; Mao, F.; Xu, Y.; Liu, J.; Wei, B.; Zhu, J.; Xiang, M.; Li, J. *Molecules* 2014, 19, 15653.
- [8] Pieczonka, A. M.; Strzelczyk, A.; Sadowska, B.; Młostoń, G.; Stączek, P. *Eur J Med Chem* 2013, 64, 389.
- [9] Kleeman, A.; Engel, J.; Kutscher, B.; Reichert, D. *Thieme Medical*, 3rd ed.: New York, NY, USA, 1999.
- [10] Wang, S.; Zhao, L.; Xu, Z.; Wu, C.; Cheng, S. *Mater Lett* 2002, 56, 1035.
- [11] Louie, J.; Gibby, J. E.; Farnworth, M. V.; Tekavec, T. N. *J Am Chem Soc* 2002, 124, 15188.
- [12] Doung, H. A.; Cross, M. J.; Louie, J. *Org Lett* 2004, 6, 4679.
- [13] Baumann, M.; Baxendale, I. R.; Ley, S. V.; Nikbin, N. *Beilstein J Org Chem* 2011, 7, 442.
- [14] Zhang, L.; Kumar, K. V.; Rasheed, S.; Geng, R. X.; Zhou, C. H. *Chem Biol Drug Des* 2015, 86, 648.
- [15] Verma, A.; Joshi, S.; Singh, D. *J Chem* 2013, 2013, 12.
- [16] Dhawas, A. K.; Thakare, S. S. *India J Chem Sec B* 2014, 53B, 642.
- [17] Toscan, C. E.; Rahimi, M.; Bhadbhade, M.; Pickford, R.; McAlpine, S. R.; Lock, R. B. *Org Biomol Chem* 2015, 13, 6299.
- [18] Prajapati, S. M.; Vekariya, R. H.; Patel, K. D.; Panchal, S. N.; Patel, H. D.; Rajani, D. P.; Rajani, S. *Int Lett Chem Phy Astron* 2014, 39, 195.
- [19] Rattan, A. *Antimicrobials in Laboratory Medicine*: Churchill BI Livingstone: New Delhi, 2000, pp. 85–108.
- [20] Li, Y.; Luo, Y.; Hu, Y.; Zhu, D. D.; Zhang, S.; Liu, Z. J.; Gong, H. B.; Zhu, H. L. *Bioorg Med Chem* 2012, 20, 4316.
- [21] Leiros, H. K.; Kozielski-Stuhrmann, S.; Kapp, U.; Terradot, L.; Leonard, G. A.; McSweeney, S. M. *J Biol Chem* 2004, 279, 55840.
- [22] Berman, H. M.; Battistuz, T.; Bhat, T. N.; Bluhm, W. F.; Bourne, P. E.; Burkhardt, K.; Feng, Z.; Gilliland, G. L.; Iype, L.; Jain, S.; Fagan, P.; Marvin, J.; Padilla, D.; Ravichandra, V.; Schneider, B.; Thanki, N.; Weissig, H.; Westbrook, J. D.; Zardecki, C. *Acta Crystallogr D Biol Crystallogr* 2002, 58, 899.
- [23] Desmond Molecular Dynamics System, version 3.7, DE Shaw Research 2014 Maestro-Desmond Interoperability Tools, version 3.7; Schrödinger, New York, NY, 2014.

SUPPORTING INFORMATION

Additional supporting information may be found online in the Supporting Information section at the end of the article.